ISSN 1330–0016
CODEN FIZBE7

CASCADE GAMMA-DECAY PROCESS OF THE ^{177}Lu COMPOUND NUCLEUS AND ITS PECULIARITIES

VALERY A. KHITROV[a], ANATOLY M. SUKHOVOJ[a], JAROSLAV HONZÁTKO[b], IVO TOMANDL[b] and GEORGY GEORGIEV[c]

[a] *Frank Laboratory of Neutron Physics, Joint Institute for Nuclear Research, 141980 Dubna, Russia*
[b] *Nuclear Physics Institute, CZ-25068 Řež near Prague, Czech Republic*
[c] *Institute for Nuclear Research and Nuclear Energy, 1784 Sofia, Bulgaria*

Received 12 June 1997; revised manuscript received 15 October 1997
Accepted 15 June 1998

From the mass of $\gamma - \gamma$ coincidences registered by a pair of Ge-detectors after thermal neutron capture in ^{176}Lu, the intensity distributions of the two-step cascades proceeding between the compound state and eight low-lying ($122 \leq E_{ex} \leq 637$ keV) levels of ^{177}Lu were obtained. The analysis of the intensity distribution of all the cascades resolved experimentally and of the total distribution, including unresolved cascades, showed that the correct description of the cascade γ-decay process for the odd-even deformed nucleus should account for the strong influence of vibrational-type excitations below 3 MeV and an abrupt transition from vibrational to quasiparticle excitations above this energy.

PACS numbers 25.40.Lw, 27.70.+q, 27.60.+j UDC 539.172.4

Keywords: compound states of ^{177}Lu, thermal neutron capture, cascade γ-decay, γ-γ coincidences, density of states, vibrational and quasiparticle excitations

1. Introduction

The systematic search for the dynamics of the of nuclear transition process from the simplest structures of low-lying levels to the extremely complex compound state was begun at the Laboratory of Neutron Physics in Dubna about 15 years ago [1,2]. To obtain a complete picture, these investigations must be performed for many nuclei with differing parameters. This will reveal both the most general properties and individual peculiarities

of nuclear states which occur in the cascade γ-decay processes following the neutron resonance capture.

The only odd-even nucleus studied thus far by the sum coincidence technique is ^{177}Lu [3]. However, statistics of $\gamma - \gamma$ coincidences in the experiment in Riga was very poor. The facility in Řež (Czech Republic) allowed a much better measurement of two-step cascades, and considerably more information on the properties of this odd-even nucleus was obtained.

2. Experiment

The $\gamma - \gamma$ coincidence measurements of the ^{176}Lu(n,γ) reaction were carried out at the LWR-15 reactor in Řež [4]. The content of ^{176}Lu in the target available was only about 0.2% (in a target of 1 g enriched in ^{175}Lu to 99.8%). However, the high capture cross-section of thermal neutrons in ^{176}Lu provided data on a sufficiently large number of the two-step cascades in ^{177}Lu. The sum coincidence method allowed the separation of the two-step cascades of a given sum energy from the mass of coincidences. Therefore, the problem of isotopic identification of the cascades was unambiguously solved on the grounds of known data on the schemes of low-lying levels and the neutron binding energies for the corresponding nuclei ($B_n = 6289.3$ keV for ^{176}Lu and 7072.4 keV for ^{177}Lu). The only drawback was that the cascades of the lower sum-energies were detected on a large background and the cascades of higher energy were obtained with the lower statistics than what could be achieved with a monoisotopic target.

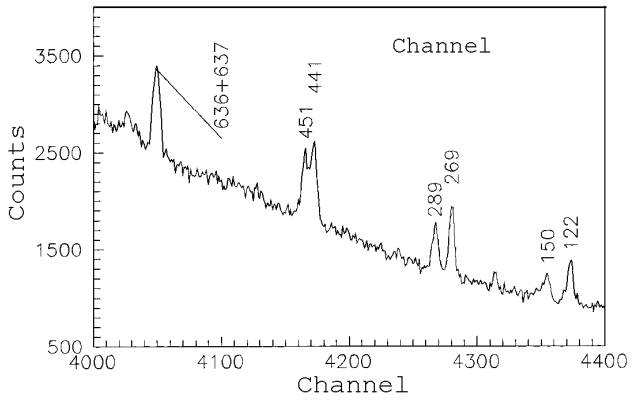

Fig. 1. Part of the sum coincidence spectrum for ^{177}Lu. *The peaks are marked by energies (in* keV*) of the final cascade levels.*

Figure 1 presents the main part of the sum coincidence spectrum of ^{177}Lu. Figure 2 shows one of the seven intensity distributions of the two-step cascades terminating at a fixed final level. The pairs of corresponding peaks in these distributions represent the most intense cascades. The conditions of their registration were carefully analysed earlier. Geometry of the experiment [1,4] was chosen so that the contribution of different errors would be minimal and would not bring to distortion larger than about 1%. Table 1 lists the tran-

sition energies, relative intensities of the two-step cascades as the percentages of the total intensity of the cascades to a given final level (including those unresolved experimentally). To reject annihilation quanta, the coincidence detection level (only for this normalization) was set at 520 keV. The relative intensities were transformed to the absolute intensities (in % per decay) by normalizing to the absolute values $I_{\gamma\gamma}$ using the relation

$$I_{\gamma\gamma} = I_{\gamma} \times br, \tag{1}$$

where the absolute intensities I_{γ} of the primary transitions with energies 6292, 5840, 5766, 5730, 5599, 5569, 5464, 5321, 5087, 5054, 4982, 4882, 4798 and 4523 keV were taken from Ref. 5. The branching ratios, br, were determined from the standard spectra of coincidences, with the primary transitions listed above, which were derived from records of coincident data accumulated in this experiment. The total absolute intensities of the cascades with a fixed sum energy are given in Table 2. The relative intensities of the cascades can be transformed into the absolute values (per 10^4 decays) by multiplying the $i_{\gamma\gamma}$ values by the corresponding $I_{\gamma\gamma}$ values from Table 2.

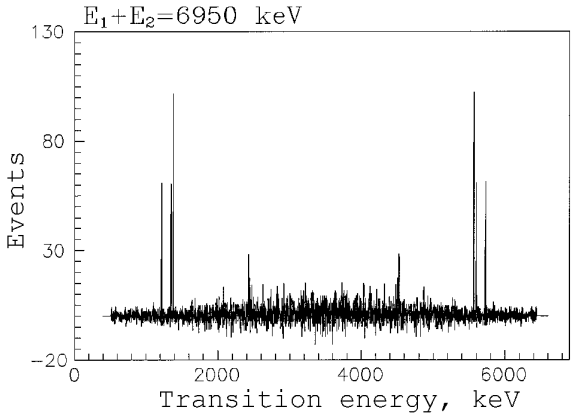

Fig. 2. Intensity distribution of the two-step cascades of total energy $E_1 + E_2$*=6950* keV*, with subtracted background.*

If at least two secondary transitions depopulating an intermediate cascade level are observed in the experiment, then the energy E_m of this level can be determined with high confidence with the use of algorithm of Ref. 6, independently of conventional methods. This algorithm uses the maximum likelihood method with the multidimensional normal distribution as the likelihood function, and is based on the obvious fact that the primary transition of the cascades proceeding via the same intermediate level is observed at the same position in different spectra. The E_m values obtained in this way are also listed in Table 1. In the case when available data did not allow unambiguous determination of E_m, the transition with higher energy was taken as the primary one. The E_m values obtained in this way are also listed in Table 1 in brackets.

TABLE 1. A list of energies, E_1 and E_2, of measured cascade transitions and their relative intensities, $i_{\gamma\gamma} \pm \Delta i_{\gamma\gamma}$, in percent of the total intensity of the two-step cascades which have the same total energy. $E_M \pm \Delta E_M$ is the intermediate-level energy. E_f is the energy of the final level of the cascades.

E_1, (keV)	E_2, (keV)	$i_{\gamma\gamma}(\Delta i_{\gamma\gamma})$	$E_M(\Delta E_M)$ (keV)
$E_1 + E_2 = 6950.8$ keV; E_f=121.6 keV			
5841.5	1109.2(6)	0.61(19)	1230.6(4)
5730.2	1220.5(1)	7.08(58)	1342.3(3)
5606.2	1344.6(4)	1.33(28)	1466.6(8)
5601.0	1349.8(1)	7.17(57)	1471.6(3)
5569.6	1381.1(0)	12.76(74)	1501.8(15)
5270.8	1679.9(6)	0.67(24)	1803.5(16)
4523.9	2426.9(2)	4.08(65)	2548.2(3)
4505.9	2444.8(5)	1.34(42)	2565.7(10)
5743.5	1207.3(6)	0.55(18)	(1328.5)
4479.0	2471.8(5)	1.16(39)	(2593.0)
3826.2	3124.6(7)	1.03(38)	(3245.8)
3795.2	3155.6(6)	1.40(44)	(3276.8)
$E_1 + E_2 = 6922.0$ keV; E_f=150.4 keV			
5905.0	1016.9(5)	1.05(34)	1167.7(4)
5842.0	1080.0(2)	3.39(50)	1230.6(4)
5607.1	1314.8(6)	1.02(35)	1466.6(8)
5266.1	1655.9(4)	1.98(49)	1806.2(10)
4983.8	1938.1(2)	3.80(67)	2089.1(6)
4962.5	1959.4(5)	1.45(45)	2108.5(16)
4780.0	2142.0(6)	1.30(41)	2290.6(15)
3966.5	2955.4(4)	3.23(82)	3106.6(10)
5815.4	1106.6(5)	1.02(30)	(1256.6)
5734.3	1187.7(3)	2.87(47)	(1337.7)
5218.2	1703.8(5)	1.61(44)	(1853.8)
5069.3	1852.7(7)	1.08(37)	(2002.7)
4943.4	1978.6(7)	1.03(38)	(2128.6)
4854.3	2067.7(5)	1.70(44)	(2217.7)
4702.7	2219.2(6)	1.32(47)	(2369.3)
4682.6	2239.4(5)	1.71(54)	(2389.4)
4667.0	2255.0(7)	1.22(45)	(2405.0)
3920.1	3001.9(8)	1.55(59)	(3151.9)
3893.1	3028.9(8)	1.56(60)	(3178.9)
$E_1 + E_2 = 6803.6$ keV; E_f=268.8 keV			
6253.9	549.7(4)	0.57(13)	818.2(4)
5605.9	1197.7(4)	0.92(21)	1466.6(8)

Table 1. (continued)

E_1, (keV)	E_2, (keV)	$i_{\gamma\gamma}(\Delta i_{\gamma\gamma})$	$E_M(\Delta E_M)$, (keV)
5601.0	1202.6(1)	6.56(47)	1471.6(3)
5569.8	1233.8(1)	4.89(39)	1501.8(15)
5393.8	1409.8(3)	1.09(23)	1676.7(19)
5171.0	1632.6(5)	0.60(20)	1901.2(4)
5164.7	1638.9(4)	0.79(21)	1907.1(13)
4965.7	1837.9(6)	0.55(18)	2108.5(16)
4798.0	2005.6(3)	1.51(31)	2274.1(4)
4789.4	2014.2(6)	0.76(23)	2284.2(10)
4782.8	2020.8(4)	0.88(25)	2290.6(15)
4524.3	2279.3(3)	2.39(42)	2548.2(3)
4374.1	2429.5(6)	0.62(23)	2697.6(6)
4363.9	2439.7(3)	1.74(35)	2708.5(4)
4214.0	2589.6(5)	1.05(32)	2858.1(4)
6296.9	506.6(7)	0.40(14)	(775.1)
5714.8	1088.8(3)	1.14(20)	(1357.2)
4987.5	1816.1(7)	0.44(16)	(2084.5)
4887.9	1915.7(4)	0.86(25)	(2184.1)
4655.8	2147.8(6)	0.72(25)	(2416.2)
4459.4	2344.2(6)	0.69(25)	(2612.6)
4394.3	2409.3(7)	0.83(30)	(2677.7)
4390.0	2413.6(6)	1.01(32)	(2682.0)
4308.5	2495.1(7)	0.66(24)	(2763.5)
4221.3	2582.3(6)	0.78(29)	(2850.7)
4201.3	2602.3(4)	1.56(38)	(2870.7)
4000.3	2803.4(6)	1.02(31)	(3071.7)
$E_1 + E_2 = 6783.4$ keV; E_f=289.0 keV			
5384.0	1399.3(5)	1.03(29)	1688.9(7)
5265.6	1517.7(3)	1.71(36)	1806.2(10)
5171.8	1611.5(7)	0.82(28)	1901.2(4)
5167.0	1616.3(7)	0.77(27)	1907.1(13)
5112.1	1671.3(2)	3.66(56)	1960.3(3)
4798.8	1984.5(6)	0.89(29)	2274.1(4)
4762.3	2021.1(5)	1.22(36)	2310.0(4)
4515.1	2268.2(7)	1.07(38)	2558.1(7)
5504.6	1278.8(7)	0.67(25)	(1567.4)
5402.0	1381.4(6)	0.80(26)	(1670.0)
5080.9	1702.5(6)	0.82(27)	(1991.1)
4816.7	1966.7(6)	0.90(30)	(2255.3)
4182.0	2601.4(6)	1.40(47)	(2890.0)
4176.1	2607.3(8)	1.10(42)	(2895.9)
$E_1 + E_2 = 6631.7$ keV; E_f=440.6 keV			
6254.6	377.1(4)	0.35(8)	818.2(4)
5730.1	901.6(2)	1.92(25)	1342.3(3)

Table 1. (continued)

E_1, (keV)	E_2, (keV)	$i_{\gamma\gamma}(\Delta i_{\gamma\gamma})$	$E_M(\Delta E_M)$, (keV)
5611.0	1020.7(6)	0.40(12)	1461.1(4)
5600.8	1030.9(2)	1.39(21)	1471.6(3)
5569.4	1062.3(3)	1.03(18)	1501.8(15)
5465.0	1166.7(1)	5.49(41)	1607.5(3)
5394.5	1237.2(4)	0.56(14)	1676.7(19)
5323.2	1308.5(2)	1.86(25)	1749.3(3)
5191.5	1440.2(5)	0.48(13)	1881.1(4)
4787.5	1844.2(3)	1.81(32)	2284.2(10)
4727.1	1904.6(6)	0.58(20)	2344.4(9)
4524.3	2107.4(2)	1.50(27)	2548.2(3)
4513.9	2117.8(4)	0.92(22)	2558.1(7)
4507.9	2123.8(6)	0.56(18)	2565.7(10)
4363.9	2267.8(6)	0.59(21)	2708.5(4)
4214.6	2417.1(3)	1.95(35)	2858.1(4)
5409.4	1222.3(4)	0.50(13)	(1662.6)
5213.8	1417.9(6)	0.40(13)	(1858.2)
5016.1	1615.6(5)	0.64(20)	(2055.9)
4744.1	1887.6(6)	0.56(20)	(2327.9)
4631.4	2000.3(5)	0.58(16)	(2440.6)
4610.1	2021.6(6)	0.46(16)	(2461.9)
4440.2	2191.5(4)	0.93(26)	(2631.8)
4406.7	2225.0(5)	0.76(23)	(2665.3)
4232.4	2399.3(5)	0.67(22)	(2839.6)
$E_1 + E_2 = 6620.8$ keV; E_f=451.5 keV			
5904.5	716.3(4)	0.43(11)	1167.7(4)
5768.8	852.0(5)	1.03(37)	1302.5(11)
5611.4	1009.4(4)	0.70(17)	1461.1(4)
5605.7	1015.1(4)	0.70(17)	1466.6(8)
5600.2	1020.6(4)	0.75(18)	1471.6(3)
5573.5	1047.3(4)	0.67(16)	1501.8(15)
5565.8	1055.0(3)	0.89(20)	1506.4(4)
5398.4	1222.4(4)	0.93(24)	1676.7(19)
5382.6	1238.2(6)	0.61(20)	1688.9(7)
5267.7	1353.1(5)	0.86(24)	1803.5(16)
5171.1	1449.7(4)	0.75(21)	1901.2(4)
5112.1	1508.7(6)	2.34(41)	1960.3(3)
4982.6	1638.3(5)	0.67(17)	2089.1(6)
4939.2	1681.6(3)	1.29(24)	2133.2(3)
4728.8	1892.0(5)	0.77(25)	2344.4(9)
4709.1	1911.7(4)	1.33(30)	2362.5(12)
6103.9	517.0(4)	0.47(11)	(968.1)
5849.2	771.7(6)	0.31(10)	(1222.8)

Table 1. (continued)

E_1, keV	E_2, keV	$i_{\gamma\gamma}(\Delta i_{\gamma\gamma})$	$E_M(\Delta E_M)$, keV
5747.6	873.3(5)	0.64(18)	(1324.4)
5328.4	1292.5(7)	0.52(19)	(1743.6)
5318.6	1302.3(4)	1.11(27)	(1753.4)
5022.8	1598.0(6)	0.54(18)	(2049.2)
4949.4	1671.5(7)	0.43(16)	(2122.6)
4883.3	1737.6(3)	1.86(35)	(2188.7)
$E_1 + E_2 = 6436.2$ keV; E_f=636.2+637.1 keV			
5771.0	665.2(5)	0.33(9)	1302.5(11)
5604.8	831.3(5)	0.51(12)	1466.6(8)
5601.1	835.1(2)	1.65(18)	1471.6(3)
5570.6	865.5(4)	0.45(10)	1501.8(15)
5566.6	869.5(7)	0.28(10)	1506.4(4)
5464.8	971.3(2)	1.37(22)	1607.5(3)
5397.2	1039.0(7)	0.39(15)	1676.7(19)
5323.0	1113.2(2)	1.33(22)	1749.3(3)
5267.7	1168.4(6)	0.43(14)	1806.2(10)
5191.2	1244.9(4)	0.68(17)	1881.1(4)
5112.0	1324.1(4)	0.86(17)	1960.3(3)
4939.3	1496.9(4)	0.71(17)	2133.2(3)
4762.5	1673.7(4)	0.96(21)	2310.0(4)
4711.4	1724.8(6)	0.49(17)	2362.5(12)
4375.2	2061.0(5)	0.86(25)	2697.6(6)
3964.7	2471.5(6)	0.89(26)	3106.6(10)
6114.6	321.6(3)	0.42(8)	(957.4)
6085.0	351.2(5)	0.27(8)	(987.0)
5528.7	907.5(3)	0.61(10)	(1543.3)
4868.8	1567.3(4)	0.64(17)	(2203.2)
4570.3	1865.9(3)	1.03(20)	(2501.7)
4530.9	1905.3(7)	0.44(15)	(2541.1)
4411.8	2024.4(7)	0.58(21)	(2660.2)
4265.4	2170.8(7)	0.59(21)	(2806.6)
4210.6	2225.6(5)	0.90(25)	(2861.4)
3991.7	2444.5(5)	0.98(27)	(3080.3)

2.1. New levels of ^{177}Lu observed in the $(\mathrm{n}, 2\gamma)$ reaction

From a comparison of the data listed in Table 1 with the available data on the decay schemes (e.g., with the NNDC file), it follows that the levels 775 (1.0), 968 (1.6), 1223 (1.0), 1257 (0.9), 1329 (0.9), 1461 (3.6), 1506 (4.4), 1567 (1.1), 1663 (1.6), 1670 (1.4), 1744 (1.7), 2123 (1.4) and 2129 (0.9) keV were not observed in previous experiments. The values given in the brackets are the absolute intensities (per 10^4 decays) of the corresponding cascades. The quanta ordering for these cascades and energies of their intermediate levels were determined in many cases on condition that the transition of the higher energy is primary. All of the possible states of ^{177}Lu listed above (except for the 1461 and 1506

keV levels) were observed for cascades whose intensities were close to the registration threshold of the experiment ($L_c \simeq 10^{-4}$). Each of the 1461 and 1506 keV levels is excited by two cascades, and these levels must be undoubtedly included in the decay scheme of ^{177}Lu. For the other cascades, we cannot exclude possibility that their primary transitions are of lower energies and that their intermediate levels are lying above 4 MeV.

The data on the levels lying above 2.2 MeV have been obtained for the first time.

TABLE 2. Total experimental, $I^{exp}_{\gamma\gamma}$, and calculated, $I^{cal}_{\gamma\gamma}$, intensities (in % per decay) of the two-step cascades in ^{177}Lu. $E_1 + E_2$ is the sum energy of the cascades; J^π_f and E_f are the spin, parity and energy of the final cascade level.

$E_1 + E_2$ keV	E_f keV	J^π_f	$I^{exp}_{\gamma\gamma}$	$I^{cal}_{\gamma\gamma}$	
				[10]	[12]
6951	121.6	$9/2^+$	1.7(1)	0.7	0.8
6922	150.4	$9/2^-$	0.9(1)	0.6	0.7
6804	268.8	$11/2^+$	2.4(2)	1.1	1.3
6783	289.0	$11/2^-$	(1.7)	1.0	1.2
6632	440.6	$13/2^+$	3.1(3)	1.3	1.5
6621	451.5	$13/2^-$	3.3(7)	1.1	1.4
6436	636.2+637.1	$15/2^+$,$15/2^-$	(2.0)	1.3	1.7
Sum			14.1(10)	7.1	8.6

2.2. Dependence of the average intensity of cascades on excitation energy

At present, no method allows the determination of the quanta ordering in the observed cascades. Nevertheless, one can approximately decompose the spectra (see Fig. 2) into two components which correspond exclusively to primary or to secondary transitions using the shape of the dependence of transition widths and level density on the excitation energy. The method of decomposition suggested in Ref. 7 is based on the fact that below some excitation energy (its value depends on the statistics of counts in the peaks of the sum coincidence spectrum; it was taken equal to 3 MeV for ^{177}Lu), the spectrum consists of:

(a) a number of well resolved discrete peaks (corresponding cascades are listed in Table 1), and

(b) a continuous low-amplitude distribution related to the large number of low-intensity cascades.

It is assumed [7] that the excitation energies of intermediate levels of the cascades satisfying the condition (a) $E_m < 3$ MeV, and for those satisfying the condition (b) $E_m > 4.07$ MeV, are determined. The intensity within the interval 3 to 4.07 MeV was divided in two parts: half was assigned to the cascades with primary energy E_1 and half to the cascades with primary energy $E_2 = B_n - E_f - E_1$. The energies of the intermediate levels of resolved cascades are listed in Table 1. In the case of unresolved cascades, these energies were determined according to the equation $E_M = B_n - E_1$. Relative intensity of both resolved and unresolved cascades was normalized using the data from Table 2.

In accordance with the procedure of Ref. 7, all seven spectra (see Fig. 2) were decom-

posed into two parts. The dependence obtained after summation of the decomposed spectra over all final levels in energy intervals of $\Delta E = 0.5$ MeV is shown in Fig. 4.

Cascades listed in Table 1 have some registration threshold L_c. For this reason, quanta ordering for a portion of the observed cascade intensities is determined incorrectly. However, one can estimate the maximum value of the sum cascade intensity for the interval $0 \leq i_{\gamma\gamma} \leq L_c$ by constructing the dependence of the cumulative sums $\sum i_{\gamma\gamma}$ of the resolved cascades on the values of intensity, and by extrapolation of this dependence to the region $i_{\gamma\gamma} < L_c$. The results of this extrapolation are shown in Fig. 3. The estimates the maximum systematical errors of the method (Ref. 7), obtained by the the extrapolation of cumulative sum to $i_{\gamma\gamma} = 0$, are shown in Fig. 4 together with statistical errors.

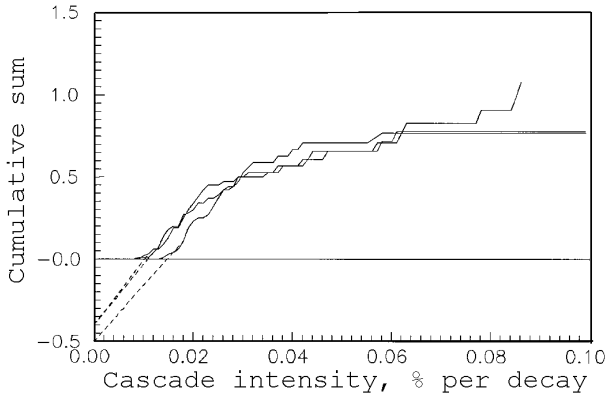

Fig. 3. Cumulative cascade intensities in ^{177}Lu *for three excitation-energy intervals:* $1.5-2.0$, $2.0-2.5$ *and* $2.5-3.0$ *MeV vs. the cascade intensity. Approximation and extrapolation of cumulative intensities to values corresponding to* $I_{\gamma\gamma} = 0$ *is shown by dashed lines.*

3. Data analysis and results

Interpretation of the cascade γ-decay of the nuclear compound states reflects the nonselectivity of the (n, γ) reaction, i.e. the rather smooth dependence on energy of the radiative strength functions and the exponential dependence of the level density on the excitation energy. The results of the calculation of the cascade intensities performed within the models of radiative widths [8,9] and level density [10] are shown in Fig. 4 by the curve 1. This figure demonstrates a considerable discrepancy between the calculations and the experimental results for the shapes of energy dependence. This discrepancy cannot be removed with any possible variation

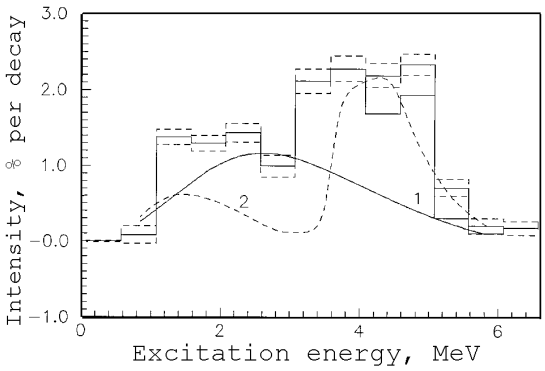

Fig. 4. Total two-step cascade intensities (in % per decay) in ^{177}Lu *as a function of excitation energy of cascade intermediate levels. The histograms represent the experimental intensities (summed in energy bins of 500 keV) with ordinary statistical errors; the maximum possible estimates of probable systematic errors are shown by additional solid curve for excitation above 4* MeV*. Curves 1 and 2 correspond to predictions according to the models of Refs. 10 and 14, respectively.*

of the model parameters [8-10]. The results shown in Fig. 4 were obtained for the cascades terminating at low-lying ($E_{ex} < 640$ keV) levels of ^{177}Lu. The data of this measurement do not allow to draw similar conclusions for the cascades to the higher-lying levels. However, the disagreement between the shapes of the calculated and experimental intensity distributions of the two-step cascades terminating at low-lying levels of the deformed nuclei studied earlier [11] is the main peculiarity of the cascade γ-decay of these nuclei. This peculiarity can possibly be related to a rather abrupt change in the functional dependence on the excitation energy:

(a) of the radiative strength functions, or

(b) of the level density of imtermediate levels in $\gamma - \gamma$ cascades.

The latter appears to be more likely.

3.1. Cascade intensities

The summed intensities of cascades leading to a set of intermediate states, $n_m =< \rho_m > \Delta E$, in the energy interval, ΔE, are calculated using the following relation:

$$i_{\gamma\gamma} = (\Gamma_{\lambda m}/\Gamma_\lambda)(\Gamma_{mf}/\Gamma_m) < \rho_m > \Delta E, \tag{2}$$

where $\Gamma_{\lambda m}$ and Γ_{mf} are the partial widths of the transitions connecting the levels $\lambda \to m \to f$, Γ_λ and Γ_m are the total radiative widths of the decaying states λ and m, respectively, and $< \rho_m >$ is the mean level density in the energy interval ΔE.

Equation (2) shows that intensities of cascades for a given energy interval of intermediate levels are mainly determined by the density of excited states of the nucleus under study. This conclusion directly follows from Eq. (2) if one takes into account that ratios of the

partial widths of the primary and secondary transitions to the total γ-widths of the states λ and m, respectively, are inversely proportional to the density of these levels. Variations of the models of radiative widths for the primary and secondary transitions affect cascade intensity considerably less [2]. Thus, the intensities of the two-step cascades are rather complex, but on the whole inversely proportional to the densities of the excited states.

Therefore, the observed disagreement between the experimental cascade intensities and the model calculations (Table 2 and Ref. 2) should be related to the fact that the observed density of intermediate levels is considerably less than the values predicted by the model of Ref. 10.

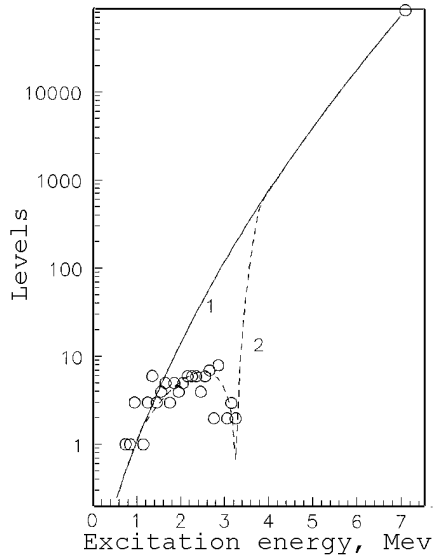

Fig. 5. Number of observed levels of the most intensive cascades in ^{177}Lu *(Table 1) for an excitation energy interval of 100* keV*. Curves 1 and 2 represent the predictions of models of Refs. 10 and 14, respectively. Histogram 3 is the estimation [12] of the level density from the shape of the distribution of cumulative sums of cascade intensities.*

The comparison between the experimental and calculated level densities for ^{177}Lu is shown in Fig. 5. The experimental data shown in this figure correspond to the cascades with $i_{\gamma\gamma} > L_c$ and cover intermediate levels with $J = 11/2, 13/2$, and $15/2$ of both parities. As can be seen in Fig. 5, a significant discrepancy between the experiment and calculations within the model of Ref. 10 is observed above the excitation energy of 1.5 MeV. Usually, such discrepancies are explained as "omission" of levels populated by cascades with $i_{\gamma\gamma} < L_c$. However, the observed intensities, which are regularly above the results of calculations, arosed doubts about the validity of the model of Ref. 10 for the considered nuclei. The authors of Ref. 12 verified it for more than 30 nuclei in the mass region $144 < A < 200$ using the data on the cascade intensities. The analysis with a minimum possible number of assumptions can be made using the summed intensities of all cascades proceeding via the same intermediate level. As shown in Ref. 12, the dispersion

of the corresponding sums is determined to more than 85-90% by the dispersion of the distribution for random intensities, i_1, of the primary transitions of cascades. Assuming that the distribution of i_1 in a sufficiently narrow energy interval follows the Porter-Thomas distribution [13] to an acceptable precision, with the mean value $< i_1 >$ and relative dispersion of 2, the authors of Ref. 12 estimated the probable number of "missing" levels in a rather wide interval of the excitation energy of heavy deformed nuclei. An approximation of the distribution of cumulative sums of cascade intensities (see Fig. 3) was used, with three main free parameters: the summed intensity, the number of cascades involved and the ratio between the mean intensities of the $E1$ and $M1$ primary transitions.

The results of the best approximation are shown in Fig. 3, and the maximum possible number of intermediate levels in ^{177}Lu for the interval from 1.5 to 3.0 MeV is presented in Fig. 5 (histogram 3).

These data, together with the data from Ref. 12, indicate that the traditional treatment of deviation of level density observed in the (n,γ) reaction from the exponential law [10] as "omission" of levels contradicts other conventional notions about this reaction such as:

(a) the non-selectivity, and/or

(b) the Porter-Thomas distribution for the reduced widths of primary transitions.

At present, it is impossible to determine whether this discrepancy is caused by the deviation of the total level density (in the present case for a fixed interval of level spins) from the exponential law of Ref. 10 and other similar models, or by the strong selectivity of the (n,γ) reaction. If the (n, γ) reaction is really selective, then the correct description of the γ-decay process can be achieved only within the framework of the model approaches which predict level density and radiative widths in the energy interval up to B_n, separately for groups of levels differing in their structure.

Namely, a model is required that would reproduce the typical dependence of the cascade intensities for deformed nuclei on the excitation energy shown in Fig. 4. It should be noted that no realistic model for the radiative strength functions is known which could reproduce the values of cascade intensities and their functional dependence on the excitation energy with hogh precision.

3.2. A simple new model of nuclear level densities

The level density model suggested in Ref. 14 assumes an abrupt change of nuclear properties due to the second-order phase transition from the boson-type excitations to the fermion-type excitations, i.e., from the vibrational excitations (phonons) to the quasiparticle excitations. The BCS-theory [15] predicts the transition from the superfluid to the normal phase for a system of Fermi particles at the critical temperature, T_c, related to the correlation function, δ, by the relation $T_c = \delta/1.76$. The level density model was developed using this relationship, and was based on the experimental data for the thermodynamic characteristics of a mixture of liquid ^{3}He and ^{4}He in the vicinity of the transition point from the superfluid to the normal state. The transition has been studied experimentally in detail [16].

After an appropriate extrapolation of the superfluid properties of the mixture of He isotopes to the number of the fermions, N_f, and the number of bosons, N_b, in the nucleus,

one can define [17] the specific heat C as a function of the nuclear excitation energy U. The specific heat is responsible for the distribution of energy of the captured neutron between fermions and bosons, and fulfils the following general requirements:

1. The specific heat of the system is equal to the sum of the specific heat of the boson and fermion systems:

$$C_{tot} = C_f + C_b. \tag{3}$$

2. In the vicinity of the phase-transition point "superfluid-to-normal state", i.e., at the critical temperature T_c, the specific heat depends logarithmically on U:

$$C_b = \alpha \ln(|U_c - U_1|) - \ln(|U_c - U|) \qquad \text{in the case of} \qquad U < U_c, \tag{4}$$

$$C_b = \alpha \ln(|U_c - U_2|) - \ln(|U_c - U|) \qquad \text{in the case of} \qquad U > U_c, \tag{5}$$

where U_c is a model parameter expressing the energy of the system at T_c. U_1 and U_2 determine the excitation energy interval where the superfluid properties can affect the γ-decay process.

For a mixture of Bose and Fermi particles, U_c must be smaller than the energy U_c^b of the phase transition for a pure Bose-condensate (pure ^{4}He system). It depends on the proportion of N_f and N_b as follows [18]:

$$U_c = U_c^b \times (1 - r)^{4/3}, \tag{6}$$

where $r = N_f/(N_f + N_b)$.

According to this model, nuclear temperature is defined as:

$$\widetilde{T} = \frac{U}{\sqrt{aU} + C_b}. \tag{7}$$

The effective nuclear excitation energy of the Fermi system is given by

$$\widetilde{U_f} = a\widetilde{T^2}. \tag{8}$$

As a consequence, the "re-determined" temperature $\widetilde{T}$ and the effective excitation energy $\widetilde{U_f}$ are smaller than the corresponding T and U values used in the conventional Fermi-gas models. Also, the level density determined according to the new model is less than what is predicted by the Fermi-gas model or by the level density model with a constant nuclear temperature.

It should be noted that the logarithmic dependence of the specific heat on energy, which appears in the new model, leads to an abrupt decrease of the level density within a narrow energy interval. The specific heat tends to infinity in the vicinity of U_c. Most probably, this situation does not completely correspond to reality because the finite size of nucleus, and the finite value of the excitation energy must restrict the increase of the specific heat. But the corresponding energy interval is rather narrow (Fig. 5). This is why one can expect that the effect under discussion does not considerably influence the calculated cascade intensity.

3.3. Comparison with experiment

Curve 2 in Fig. 4 represents the results of the calculation within the model of Ref. 14. As seen in the figure, the model reproduces reasonably well the shape of the cascade intensity distribution and improves the quantitative agreement. The model parameters used in the calculation are: $U_1 = 1.2$ MeV, $U_2 = 3.84$ MeV, $\alpha = 1.3$ and $r = 0.45$. They are in a good agreement with the corresponding values obtained for other nuclei.

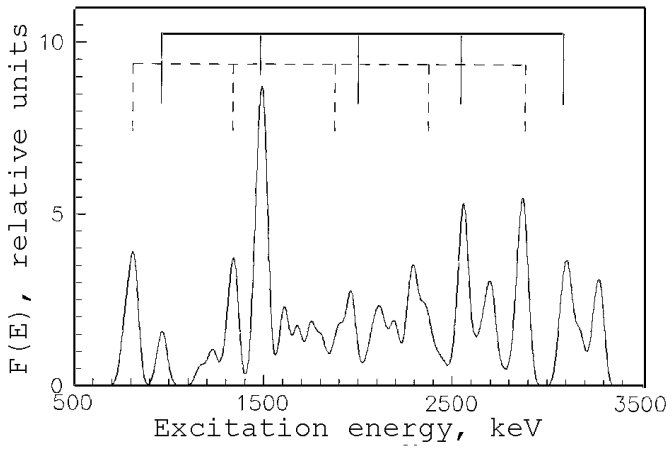

Fig. 6. The dependence of the intensities (% per decay) of the resolved cascades listed in Table 1 on the excitation energy. Possible "bands" of practically harmonic excitations of the nucleus are marked. The parameter $\sigma = 25$ keV *was used.*

Table 2 compares the total intensities calculated within the models of Refs. 10 and 14 (in % per decay) to the experimental values for the two-step cascades. The calculations were performed for the compound state with $J^\pi = 13/2^-$. As can be seen from the table, the model suggested in Ref. 14 provides a better agreement with the experimental data than the model of Ref. 10. However, in order to reach a reasonable correspondence between the experiment and calculations within the new model, it is necessary to lower the level density above the excitation energy of 3 MeV and/or to increase the widths of the secondary transitions to the lowest-lying levels (this should primarily be done for cascades to levels of positive parity).

The main discrepancy between the model of Ref. 14, and the conventional models about the level density and the radiative strength functions, is mainly in the predicted values of the level density. The effects of superfluidity (i.e., of the re-determination of nuclear temperature) on the model $E1$ transition widths [8] and on the cascade intensities are very small.

Figure 5 shows the numbers of the observed levels in 100 keV energy intervals as a function of the excitation energy. Experimental data (points) are compared with the predictions of the conventional back-shifted Fermi-gas model [10] and of the model of Ref. 14.

As can be seen from Fig. 5, the simple model of Ref. 14 reproduces the experimental data rather well up to the excitation energy of 3 MeV (without the use of a considerable omission of levels that are weakly excited in the cascade transitions). Since this model assumes (on the basis of the available data) the dominant influence of phonon excitations below the energy of 3-4 MeV on the γ-decay probability of the even-N deformed nuclei, it would be worthwhile to find an independent confirmation of this effect. This phenomenon can appear as a regularity in the region of intermediate levels fed by the most intensive cascades.

A very simple method allows the study of this regularity. The absolute intensities of individual cascades (see Tables 1 and 2) are smoothed in the vicinities of their intermediate-level energies E_m by the Gaussian curve with the parameter $\sigma = 25$ keV. The sum of these distributions over the total number of experimentally resolved cascades gives the spectrum $f(E)$ of the smoothed cascade intensities. The distorting influence of the global energy dependence of the cascade intensities involved in the analysis was considerably reduced by the normalization $F(E) = f(E, \sigma)/f(E, \sigma = 250 \text{ keV})$, where the spectrum $f(E, \sigma = 250$ keV) is constructed from the same set of cascades. The spectrum $F(E)$ is shown in Fig. 6 as a function of the excitation energy. As can be seen from the figure, the spacings between the most intense peaks in this distribution are almost equal and the peaks can be placed in practically equidistant "bands". The search for the equidistant period T was performed by means of the autocorrelation function

$$A(T) = \sum_E (F(E) \times F(E+T) \times F(E+2T)) \tag{9}$$

with the summation over the excitation energy E. Figure 7 demonstrates the values of the functional $A(T)$ for different periods T of the expected equidistance. The two curves in this figure correspond to different detection thresholds of the cascades. It follows from Figs. 6 and 7 that the intermediate levels of the most intense cascades in ^{177}Lu can be placed in one or more "bands" with the most probable equidistant period of T=530 and/or 600 keV. These "bands" are marked in Fig. 6.

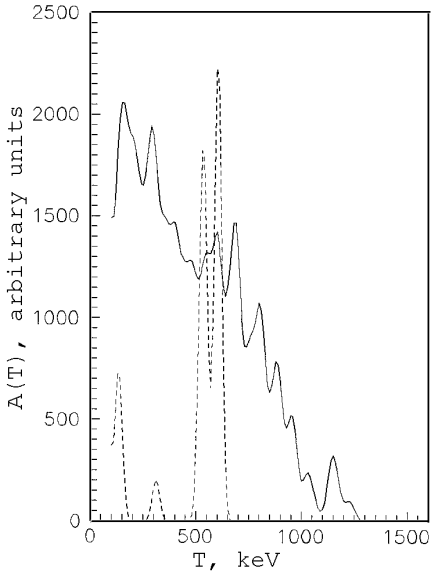

Fig. 7. The values of the functional $A(T)$ for the two registration thresholds of the most intense cascades: the solid curve corresponds to all resolved cascades listed in Table 1; the dashed curve corresponds to cascades with intensities higher than 0.1% per decay.

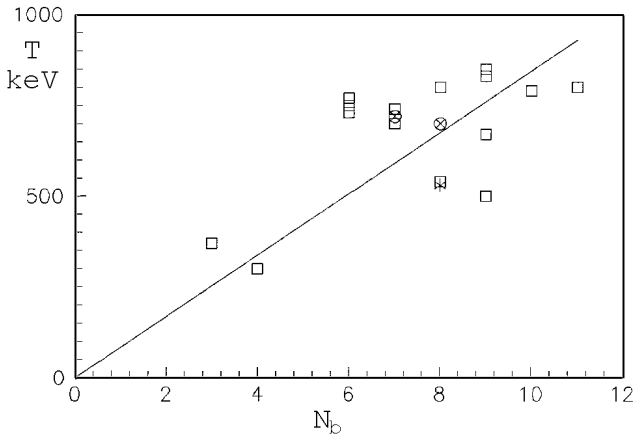

Fig. 8. The value of the equidistant period, T, for ^{177}Lu (asterisk) and even-even nuclei studied earlier (rectangles) as a function of the number of boson pairs, N_b in the unfilled shells. The $\otimes$ show the ϵ_d values for the ^{110,112}Cd nuclei. Line extrapolates the possible dependence.

It should be noted that the problem discussed here can not have an unambiguous solution [19] if only the data on cascades following thermal neutron capture in a single nucleus

are taken into consideration. The final conclusion about the confidence level of the observed regularity can be made only after studying the two-step cascades from different resonances for a large set of nuclei.

An additional argument in favour of the nonrandom nature of the observed regularity of the enhanced cascades in ^{177}Lu follows from an analysis of the T values determined in the described way for a group of even-N nuclei [19]. Figure 8 presents the value of the obtained equidistant period versus N_b for the even-N nuclei. It can be seen that the results of this analysis allow for the possibility of finding the linear dependence $T = kN_b$ and that the value of T for ^{177}Lu is in a rather good agreement with this empirical dependence [20].

4. Conclusions

The analysis of the experimental data on the two-step cascades proceeding between the compound state and eight low-lying levels of ^{177}Lu shows that the γ-decay process of this odd-even deformed nucleus reveals the same main peculiarities as those observed earlier for the even-even, even-odd and odd-odd deformed nuclei. These results support the previous assumptions about the factors affecting the γ-decay:

(a) a rather abrupt change of the nuclear properties at the excitation energy of about 3-4 MeV;

(b) a possible dominance of vibrational-type excitations below this energy which results in a strengthening of the widths of the cascade transitions to the low-lying levels of the ^{177}Lu nucleus. The greatest strengthening can be related to the practically harmonic nuclear vibrations having a phonon energy of about 530-560 keV.

Acknowledgements

Authors' thanks are due to Ms. Ann Schaeffer for her help in preparation of the English version of this paper. This work was supported by GACR under contract No. 202/96/0551 and by RFBR Grant No. 95-02-03848.

References

1) S. T. Boneva, E. V. Vasilieva, Yu. P. Popov, A. M. Sukhovoj and V. A. Khitrov, Sov. J. Part. Nucl. **22(2)** (1991) 232;

2) S. T. Boneva et al., Sov.J. Part. Nucl. **22(6)** (1991) 698;

3) M. R. Beitins, V. A. Bondarenko, I. L. Kuvaga, L. H. Khiem, Yu. P. Popov, P. T. Prokofjev, A. M. Sukhovoj, V. A. Khitrov and Yu. V. Kholnov, Izv. RAN, Ser. Fiz. **57(1)** (1993) 36;

4) J. Honzátko, K. Konečný, I. Tomandl, J. Vacík, F. Bečvář and P. Cejnar, Nucl. Instr. and Meth. **A376** (1996) 434;

5) Nuclear Data Tables **Vol. 26(6)** (1981) 511;

6) Yu. P. Popov, A. M. Sukhovoj, V. A. Khitrov and Yu. S. Yazvitsky, Izv. AN SSSR, Ser. Fiz. **48** (1984) 1830;

7) S. T. Boneva, V. A. Khitrov, A. M. Sukhovoj and A. V. Vojnov, Z. Phys. A **338** (1991) 319;

8) S. G. Kadmenskij, V. P. Markushev and W. I. Furman, Sov. J. Nucl Phys. **37** (1983) 165;

9) J. M. Blatt and V. F. Weisskopf, *Theoretical Nuclear Physics*, McGraw-Hill, New York (1952);

10) W. Dilg, W. Schantl, H. Vonach and M. Uhl, Nucl. Phys. **A217** (1973) 269; T. von Egidy, H. H. Schmidt and A. N. Behkami, Nucl. Phys. **A 481** (1988) 188;

11) S. T. Boneva, V. A. Khitrov, A. M. Sukhovoj and A. V. Vojnov, Nucl. Phys. **A589** (1995) 293;

12) A. M. Sukhovoj and V. A. Khitrov, Yad. Fiz., to be published; JINR preprint P3-97-223 (in Russian);

13) C. F. Porter and R. G. Thomas, Phys. Rev. **104** (1956) 483;

14) S. T. Boneva, V. A. Khitrov, Yu. P. Popov and A. M. Sukhovoj, Proc. of IV International Seminar on Interaction of Neutrons with Nuclei (Dubna, 1996) E3-96-336, Dubna (1996) 183; S. T. Boneva, V. A. Khitrov, Yu. P. Popov and A. M. Sukhovoj, In Capture Gamma-Ray Spectroscopy and Related Topics, Budapest, Hungary, October 1996, Vol. 1, p. 483;

15) J. Bardeen, L. Cooper and J. Schrieffer, Phys. Rev. **108** (1957) 1175:

16) F. Gasparini and M. R. Moldover, Phys. Rev. Lett. **23** (1969) 749;

17) M. Sano and S. Yamasaki, Progr. Theor. Phys. **29** (1963) 397;

18) E. C. Kerr, Proc. LT-5, Madison (1958) p. 158;

19) E. V. Vasilieva, A. V. Vojnov, O. D. Kestarova, V. D. Kulik, Yu. P. Popov, A. M. Sukhovoj, V. A. Khitrov, Yu. V. Kholnov and V. N. Shilin, Bull. Russian Acad. Science, Physics **57** (1993) 1582;

20) V. A. Khitrov and A. M. Sukhovoj, In: *Nuclear Data for Science and Technology*, eds. G. Refo, A. Ventura and C. Grandi, ICTP, Trieste, May 1997, p. 750.

KASKADNI GAMMA RASPADI SLOŽENE JEZGRE ^{177}Lu I NJENE POSEBNOSTI

Na osnovi velikog broja $\gamma - \gamma$ sudesa od uhvata termičkih neutrona u ^{176}Lu, zabilježenih pomoću dva Ge-detektora, izvedene su raspodjele intenziteta kaskada parova fotona od prijelaza sa stanja složene jezgre preko međustanja na osam niskih ($122 \leq E_{ex} \leq 637$ keV) stanja ^{177}Lu. Analiza svih raspodjela intenziteta prijelaza koji su bili razlučeni i ukupne raspodjele, uključivši i nerazlučene kaskade, pokazuje da opis kaskadnih γ-raspada ove deformirane neparno-parne jezgre mora uzeti u obzir snažan utjecaj vibracijskih uzbuđenih stanja za stanja ispod 3 MeV, te nagao prijelaz od vibracijskih ka kvazičestičnim stanjima iznad te energije.